ROMANIAN JOURNAL OF INFORMATION SCIENCE AND TECHNOLOGY
Volume **16**, Number 1, 2013, 29–51

Improved Heterogeneous Gaussian and Uniform Mixed Models (G-U-MM) and Their Use in Image Segmentation

Horia-Nicolai TEODORESCU[1,2], Mariana RUSU[3]

[1] "*Gheorghe Asachi*" Technical University of Iaşi Romania, Ic si, 8 Bd. Carol I
[2] Institute of Computer Science of the Romanian Academy, Romania, Iaşi
E-mail: hteodor@etti.tuiasi.ro

Technical University of Moldova, R. Moldova,
Chişinău, Bd. Ştefan cel Mare, 168
E-mail: mrusu@etti.tuiasi.ro

Abstract. Recently, the combined Gauss Mixture and Uniform Distributions Mixture Model, shortly Gauss-Uniform Mixture Model (G-U-MM) was proposed to better relate to the nature of a complex distribution and to simplify the characterization of processes that need too many Gauss functions in a standard Gauss Mixed Model (GMM). For a reasonably large class of images, the Gauss-Uniform distribution mixed models are easier to apply than the GMM models because the former ones produce significantly smaller numbers of elements in the mixture. The method has solid mathematical foundation and might be better related to the processes of image segmentation performed by humans. In addition, while computationally simple, it produces remarkable results. We discuss supplementary reasons for the use of the G-U-MM heterogeneous models in image segmentation and improve the previously presented algorithm of segmentation by removing the possible confusion between sections of Gaussian distributions and intervals of uniform distribution. Consequently, the approximation precision of the histogram and the segmentation are improved. Several examples illustrate the algorithm performance.

Key words: image segmentation, Gaussian Mixture Model, Gaussian-Uniform Mixture Model, evaluation of segmentation.

1. Introduction

Image segmentation aims to determine in a picture the relevant "objects" and "elements" that have significance for the human observer. Typically, in a picture, the number of such objects is small and include, beyond the background, one or several landscape features, as trees, animals, man-made artifacts as houses and details of buildings, other traces of human activity, and humans and their details, as face details, clothing, and objects carried by humans.

Segmentation poses several challenges, as the number and type of relevant elements depend on the purposes of human observation, mixing utilitarian and semantic scope with local and global geometrical, statistical and textural properties of the image. Tests performed on large groups of subjects asked to perform segmentation of the same images show that segmentation results produced by humans may differ significantly, see the database database [33]. Therefore, it cannot be expected that a single segmentation procedure would yield a globally satisfactory result. This explains the large number of segmentation methods presented in the literature, as region-growing method [1], [2], split and merge [3], clustering methods (k-means, fuzzy C-means [4]), edge-based segmentation [5]; thresholding – segmentation based on classification of pixels according to their intensity [6], [7], based on graphs [8], wavelets, and other hybrid methods (*e.g.*, [9]).

We believe that there are several simple and general properties of the segments that probably are used in the human segmentation process that can be transposed in automatic segmentation procedures. We suggest that such properties are the type of probability density function (p.d.f.) and the type of texture. For example, the eye would detect when the statistics is essentially of Gaussian type or of uniform type. Also, we suggest that the eye tends to merge sub-segments when their statistics is different but whose texture is similar, or vice-versa. The idea is not to have a very large set of segments, many of them devoid of meaning for the human observer, but a minimal number of segments that are of interest. For example, segmenting a meaningful element in the scene because of shades of light should be avoided, by combining the respective sub-segments in a single one. In this respect, the typical decomposition models as Gaussian Mixtures Models (GMM) are deficient, as they tend to produce a large number of segments based on minute differences in gray level statistics. Our use of local averaging of the histogram contributes to eliminating such small differences and to producing larger segments with almost Gaussian approximations. There are four key ideas in this paper:

i) The use of a mixture of Gaussian and uniform distributions for approximating the distribution of gray levels in images, instead of pure Gaussian mixtures. This approach is named Gauss-Uniform Mixture Model (GUMM).

ii) The use of an interval-wise (piecewise) approximation of the gray levels distribution in the frame of GUMM.

iii) The image segments are determined by the gray-level intervals found in the piecewise GUMM approximation.

iv) The GUMM approximation is performed by a heuristic algorithm with low computational demands.

The remaining part of the paper is organized as follows. Section 2 reviews the fundamentals of the Gauss mixture model (GMM), makes a critics of the previous version of the GUMM algorithm proposed by the authors, discuss the relation between semantic content of the images and their segmentation, shows the rationale of using GUMM, and briefly looks at several technical aspects of segmentation and of the GUMMs. The third Section introduces the principle of the new heuristic GUMM algorithm, while Section 4 presents the algorithm and its variants. The results are summarized in Section 5. The quality of the segmentation is analyzed in Section 6. The last Section is conclusive.

2. Fundamentals

2.1. GMM versus G-U-MM

The Gaussian Mixture Models (GMMs) were recently widely used in relation to approximation of functions and specifically of probability density functions. Among the frequently cited applications of GMMs are speech recognition [10], [11], detection of emotions in speech [12], and image analysis and segmentation [13], [14].

These models rely on the fact that the family of Gaussian functions is a complete family for the set of derivable and bounded functions $f : \mathbf{R} \to \mathbf{R}$. It is well known that "both classification and regression can be viewed as function approximation problems" [15]. That means that segmentation, which is a specific type of clustering, can be reduced to approximation. Pure Gauss Mixture Models may require a large number of Gauss functions for performing a reasonable approximation when the statistics (probability density function, p.d.f.) of the approximated process has large regions (intervals) where the p.d.f. is almost constant. A simple example is the uniform noise process, which requires a huge number of superposed Gauss functions to approximate it reasonably well in a GMM model. The heterogeneous G-U-MM was first used in relation with image segmentation and explained in some detail in [15], [16]. In this paper, we review the model, enhance the algorithm, discuss in detail the application to image segmentations, and propose extensions to other heterogeneous models.

One of the disadvantages of the approach presented in the previous papers [14], [17] is that the top section of the Gaussians, when they are large enough (wide, spread Gaussians), are wrongly determined as constant intervals and transformed into false uniform (U) segments. Removing from the data those intervals also creates difficulties in the true GMM representation that were meant to stand for those regions. We improve on that drawback of the method in [14], [17] by adding conditions for eliminating that deficiency. In the remaining part of the paper, we use histograms for approximating probability densities functions. In addition, we deal with smoothed histograms. Subsequently, throughout the paper, 'histogram' will actually mean smoothed histogram.

2.2. Semantics and approximation in image segmentation

Various segmentation procedures have been proposed during the last five decades. Some of them are based on simple statistical characteristics of the image mentioned in [1]-[3], [5]-[7], [25], on more elaborate features based on fuzzy-logic descriptions of the image properties [4], [6], or *ad hoc* features, as determined for example by neural networks [18]. None of these methods yielded completely satisfactory results compared to human segmentation. The problem may have the root in the different ways humans and the proposed segmentation algorithms operate, or in the seeking of algorithms based on simplified, but mathematically "elegant" methods of segmentation.

Gaussian mixture models (GMMs) are abstractions that are convenient from the mathematical point of view. Indeed, GMMs represent a mathematically nice way of producing a distribution with respect to a complete set of functions, in the space of statistical distributions. The question is if this decomposition relates well to the semantics (ontology) used by humans in the segmentation and to shape recognition process.

Image segmentation by humans achieves detection of salient elements in an image. Unessential details are skipped, reducing the recognition process to semantically rich elements. We suggest that statistics and texture, the last one being perhaps predominantly detected through gradients and through statistical moments, are used by the human eye to detect "objects", that is, segments, in images. Some dynamical form of reconfiguring the image for abstracting semantically salient elements (segments) is probably performed by the human mind. The use of statistics in the similar way the human mind is doing presupposes a mechanism that is based on recognizing simple characteristics of the statistics, as constant gray values, constant gray level distributions (uniform noise-like, uniform distribution), almost linearly varying gray levels, and white noise (Gauss distributions). This supposed way of human object recognition, complemented by contours recognition, elicits a method of segmentation rooted in the decomposition of the histograms in the main regions with statistics that are almost the same to specific, simple distributions, as constant distribution (uniform-like) and white noise distribution.

2.3. Rationale of using G-U-MM in image segmentation

As already noted, the main role of image segmentation is the discovery in images of elements that are hopefully meaningful to the human interpreter and the obtaining of a simplified image, with fewer gray levels, that reduces to those essential elements of the initial image. For human observers, it seems that segmentation may be a relatively natural stage in image perception; however, how much pattern recognition is involved in the human image segmentation is unclear. Therefore, trying to base a technical method of segmentation only on basic image processing techniques, with no higher-level knowledge on the image properties and with no feedback applied after potential patterns are discovered may be impossible when the identified segments are required to connect to meanings.

There is no obvious connection between segments in the image and the compo-

nents in the pixel gray level distribution; in fact, the connection is not direct. Therefore, the use of GMMs or other similar models in image segmentation may look a wrong technique to use. However, some basic assumptions, frequently verified experimentally, as we empirically found out in numerous experiments, connect the use of GMMs and G-U-MMs to segments in images. In the first place, in images that are not overcrowded by objects, semantically significant elements in the image are frequently rather well approximated by Gaussian components. Therefore, identifying the Gaussian components correctly helps in getting the segments. Secondly, large sections of the background as well as several semantically significant elements in the image have frequently almost uniform gray level, meaning that their distribution is uniform. Consequently, local statistics that pertain to Gaussian-like or uniform-like distributions tend to be meaningful for the segmentation process. The presence of these regions (see Fig. 1 – Fig. 4) shows that only-Gaussian models are not good enough, because they actually miss the regions with uniform-like distributions of the gray levels. Modeling uniform-like distribution with GMMs, while feasible, represents a poor approximation method because it requires a large number of Gaussians. The empirical evidence thus suggests that a mixture of Gaussians and uniform distributions would allow a simpler, computationally less expensive, and, most importantly, much easier to interpret decomposition of the image in meaningful segments.

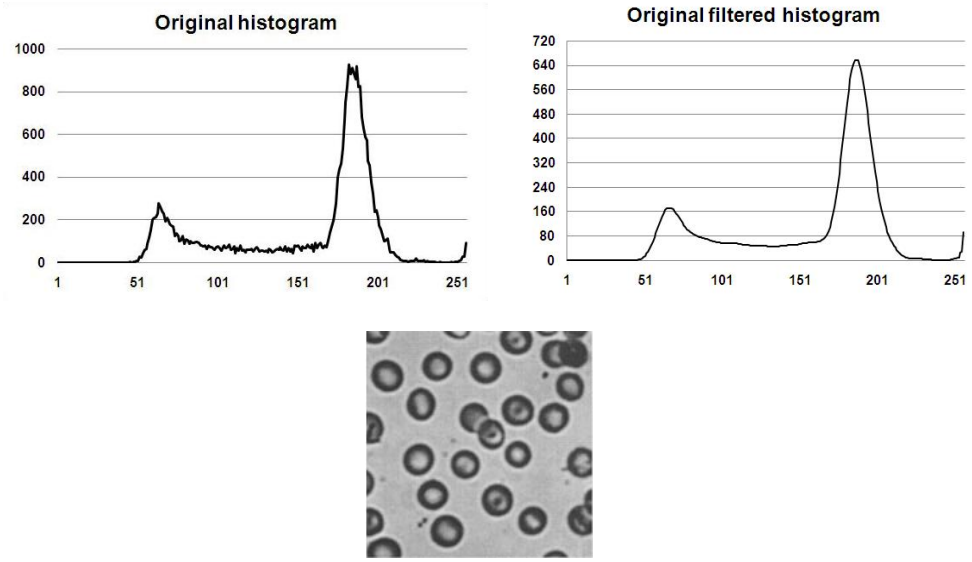

Fig. 1. Typical histogram (of test image *Blood cells* [19] 170×170 pixels) easily decomposable into one large constant interval in the middle and two Gauss functions. The first Gauss distribution seems superposed with the first uniform distribution (UD), but not with the second.

The perspective on image decomposition presented above shows that i) there is no reason to believe that the GMM method is a suitable way to detect segments in

an image; ii) in fact, there is evidence proving that GMM may be computationally intensive and non-optimal for several classes of images; iii) we cannot expect to obtain human-like segmentation with methods based solely on p.d.f. decomposition when texture plays a role in the definition of the segments and when pattern recognition processes are used by the human to perform segmentation. In this paper, we focus on the first two issues, (i) and (ii) above.

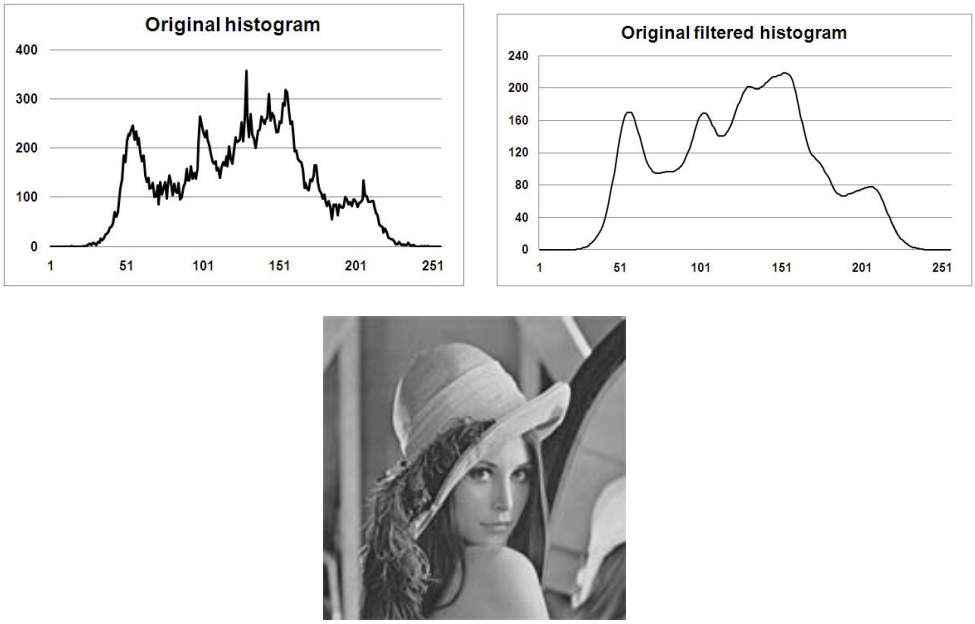

Fig. 2. Typical histogram (of test image *Lena* [20] 170×170 pixels) best modeled by a Gaussian Mixed Model (GMM). The smoothed version of the histogram is clearly perceived as composed of a Gaussian mixture.

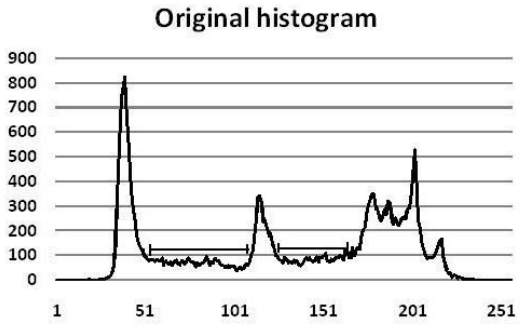

Fig. 3. Histogram of the gray level version of the picture of one of the authors (available at `http://www.fict.ro/HNT.htm`). Notice the two segments where the distribution (histogram) is almost constant.

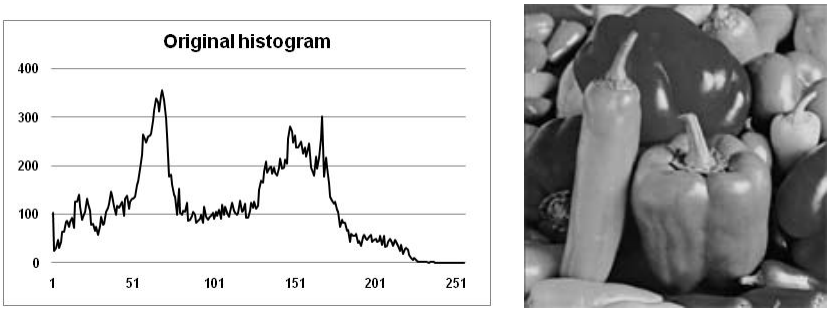

Fig. 4. Histogram(of test image *peppers* [21] 170×170 pixels) of the gray level version of the picture of the peppers. Notice that the central interval on the histogram is an almost constant probability one.

2.4. Segmentation based on p.d.f decomposition as an optimization problem

The discussion in this section relates to the general topic of the segmentation through the next assumption:

An image segmentation based on the linear decomposition of its p.d.f. according to a set of specified functions is correct (acceptable for whatever purpose.)

This is only a working hypothesis. As we already emphasized, the hypothesis is disputable at best and false at worst. Denote by $f(g)$, the p.d.f. of the image, where g is the gray level and f is a continuous function $f : \mathbf{R} \to \mathbf{R}$. Consider that the segmentation is based on a decomposition of f according to a set Ω of functions. (The reader is referred to functional analysis books for the basic notions in this section.) We assume that Ω is a complete family of functions for the space of continuous real valued functions on $\mathbf{R}$, that is, for any f, there is a (possibly infinite) subset of Ω, $\Omega_f \subset \Omega$ and a set of real numbers, a_k, such that $f(g) = \sum_k a_k \omega_k(g), \omega_k \in \Omega(f)$. For now, we assume that the set Ω is specified. A finite approximate representation of f is a sum of a finite number of functions ω_k, $\tilde{f}(g) = \sum_{j=1..n} a_j \omega_j(g)$. In the framework of the segmentation task, each function $a_j \omega_j$ in the finite decomposition represents a segment. We do not question here the suitability of assigning the meaning of 'segment' to the functions $a_j \omega_j$.

The function $\tilde{f}$ is an approximation, with some error, of f. Suppose that we are interested in the square error of the global approximation. We stress again that this optimality criterion has nothing in common with the achievement of a specified segmentation. The square error of the global approximation is defined as

$$\varepsilon^2(f, \tilde{f}) = \int_{g1}^{g2} \left(f(g) - \tilde{f}(g)\right)^2 dg, \tag{1}$$

where g_1, g_2 are the limits of the gray interval. In the framework of the approximation problem, computationally, the optimal solution of the approximation is that that

achieves an approximation with an error lower than a specified value, ε_0. Using the expression of the finite decomposition, for a specified set of n indices, $j_1, j_2, ..., j_n$, one has

$$\varepsilon^2(f, \tilde{f}) = \int_{g1}^{g2} \left(f(g) - \sum_{j_1,...,j_n} a_k \omega_k(g)\right)^2 dg. \tag{2}$$

The problem becomes: Find q such that it is the smallest number of functions ω_k needed to make the error less than ε_0. While formally the above condition is simple, its application may not be so. It is one of the reasons we prefer a heuristic solution. The problem is simple only when one can easily determine the principal component decomposition of f.

2.5. G-U-MM as additive models

The proposed G-U-MM falls into the well-known category of additive models [23], where the model is applied to the distribution function

$$f(x) = f_1(x) + f_2(x) + ... + f_n(x).$$

The model, under some hypotheses [16], may be also suitable for models of signals in the form $X = S + N$, where S is a signal in a lower-dimensional space E than the process X, and N is an independent Gaussian noise with null average and noise covariance matrix [16].

This brings us to three entirely different problems, the first related to the filtering of the image (noise removal), the second to the filtering of the histogram (histogram smoothing), and the third to the segmentation.

Relating to the first problem, notice that, because we assume that the additive noise has zero mean for the pictures to analyze, we suggest that a repeated, small window average filtering significantly reduces the noise N. When salt and pepper noise is present, a mixture of repeated average and median filters may clean enough the signal. Details on this preliminary filtering procedure are provided in [14]. Therefore, we will consider subsequently that the only process we deal with is segmentation.

The images however may include 'semantic noises', that is, small objects that actually occur in the image but are of no meaning for the viewer. Such 'semantic noise' is removed by smoothing of the histogram. Yet, 'semantic noise' may include strong shades and details of the background that are details devoid of interest, or details of the background and shades that are overlapping with parts of the "interesting signal" and that have identical or close gray levels (or colors) with the "interesting" objects in the image.

Regarding the additive model (additive in distributions) referring to segments, in this paper we make the assumption that each of the functions f_k, in this specific additive model, are not zero on an interval where all other functions, $f_{j\neq k}$, are null (that is, piecewise decomposition). Only the latter meaning of additive model is pursued subsequently.

3. Heuristic G-U-MM algorithm

3.1. Limits and improvements on the basic G-U-MM

Some of the basic assumptions we put forth are not verified. In the first place, we suppose that the eye recognizes images using both gray levels and texture. Texture can be typically characterized using third order statistics in conjunction with second order moments, while we take into account only the basic statistic (p.d.f.).

The additive model $f(x) = f_1(x) + f_2(x) + ... + f_n(x)$ is the same either if the composing functions have the same definition domain, or if represents extensions to a common definition domain of functions that have disjoint definition domains. While formally this distinction is immaterial, algorithmically significant simplifications can occur in the second case, while semantically the difference in segmentation may be noteworthy.

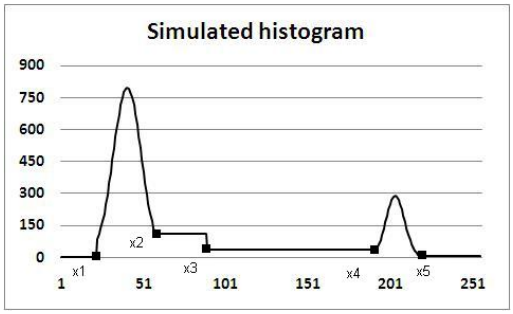

Fig. 5. Simulated histogram composed of two uniform and two Gaussian distributions.

An example of realistic histogram may look as in Fig. 5. The histogram is composed by a sum of four components (not taking into account the intervals below x_1 and above x_5. The second and the third are two superposed uniform distributions

$h(x) = u_3(x) + u_4(x)$,

where the distributions have the form

$u_3(x) = a_3$ for $x \in [x_2, x_3]$, 0 otherwise

$u_4(x) = a_4$ for $x \in [x_3, x_4]$ 0 otherwise

The first and the fourth components are Gaussian. On the remaining intervals of the gray interval, where h is not constant (not uniform distribution), h is modeled by Gaussian mixtures. The final result is composed of the set of marked intervals corresponding to uniform and "Gaussian" distributions. To each such interval, a segment gray value is assigned, where the segment value is the average gray value in the interval. As presented in the preliminary papers [14], [17], preprocessing and basic analysis steps are performed on small sliding windows (up to 24 gray values). At this stage of mixture analysis, for intervals narrower than two windows, we split them in two equal intervals and connect these to the adjoined intervals.

3.2. Avoiding the false interpretations of Gaussian segments as 'uniform distribution' segments

For avoiding the classification of the top of the Gaussians with a large spreading as locally uniform distribution, we use a semi-empirical method and the related algorithm described in this section. The method is semi-empirical because we do not aim to determine the true (precise) Gaussian decomposition for the given interval. Instead, we aim to test if a rough approximation by a Gaussian on the interval does not perform well enough, then extend the approximation to a larger interval to see if the approximation behaves better than a uniform one. When the result is better for the rough Gaussian approximation, we decide that the interval belongs to a Gaussian section of the histogram.

We perform a rough Gaussian approximation on all intervals with uniform distribution (UD). Namely, for each UD interval obtained from the UD test explained in the previous papers [14], [17] we take the middle of the respective interval and determine a tentative spreading from the equation that relates the value of the Gaussian, the accepted error for constancy, and the width of the interval,

$$A(1 - e^{-(x-m)^2/2\sigma^2}) \leq \epsilon, \tag{3}$$

where ϵ is the error used in the criterion, m is the middle of the interval determined as UD, σ is the assumed spreading of the assumed Gaussian, and x is one of the extremities of the interval. The factor A is the peak of the value in the interval; to further remove the noise effect, it is determined as the average of the three largest values in the interval. We solve the case of equality for the above and determine σ^2 as:

$$1 - \epsilon/A = e^{-(x-m)^2/2\sigma^2}. \tag{4}$$

After taking the logarithm, we obtain:

$$\sigma^2 = -(x-m)^2/(2\ln(1-\epsilon/A)). \tag{5}$$

Two values of σ are obtained, each for one extremity of the false UD interval, denoted here by $[x_1, x_2]$. Namely, the two values are:

$$\sigma_{1,2}^2 = -(x_{1,2} - m)^2/(2\ln(1-\epsilon/A))$$

We assume that the value m corresponds to the peak of the histogram in the interval, $m = argmax_{(k)}(h_k)$, where h_k denotes the k^{th} value of the histogram. (When the estimation is correct, $m = argmax_{(k)}(h_k)$ is indeed the average value according to the Gaussian.) We take the average $(\sigma_1 + \sigma_2)/2$ as the value for σ. Then, we compute the average square error for the approximation with the obtained Gaussian. If this error is lower than the average square error determined in the respective interval using the constant value approximation, we decide that the interval is not uniform, but part of a Gaussian. In this case, the false UD segment is merged with the adjacent segment.

The algorithm for determining if an apparent UD interval is in fact the cap of a Gaussian with large spreading is as follows. Assuming that the Gaussian (if it is actually present) is not too noisy, then:

1. Choose a UD interval $[k_1, k_2]$ and determine the maximal value inside it, $max_k h_k$, and the corresponding value of k, k_m. If $|k_m - (k_1 + k_2)/2| < \epsilon(k_2 - k_1)$, then decide that k_m is the centre of the Gauss function. If not, determine the three highest values in the interval $[k_1, k_2]$ and determine their average. Apply the centrality test to the average.

2. If the centrality test is not satisfied, stop: the interval $[k_1, k_2]$ is an UD interval, or is of unknown type, but we force the approximation by an uniform distribution.

3. If at least one centrality test is satisfied, then determine σ_1, σ_2 and σ, as explained above.

4. Compute the square error for the Gauss function hypothesis,

$$\varepsilon_G^2 = \sum_{k=k_1}^{k_2} (G_k - h_k)^2 \tag{6}$$

   where G_k denotes the value of the Gauss function at point k; compute the square error for the UD hypothesis

$$\varepsilon_U^2 = \sum_{k=k_1}^{k_2} (C - h_k)^2 \tag{7}$$

   where C is a constant represented by the average of the values in the interval, and ε_U^2 is the standard deviation in the interval.

5. If $\varepsilon_G^2 < \varepsilon_U^2(1 + \epsilon_{G-U})$, where ϵ_{G-U} is a small quantity (for example, 0.5), tentatively decide that the interval corresponds to a Gaussian.

6. If the interval corresponds to a tentative Gaussian, expand the interval with one sample to the left. Compute again on the new interval new values for ε_G^2 and for ε_U^2. If $\varepsilon_G^2 < \varepsilon_U^2(1 - \epsilon_{G-U})$, decide that the initial interval belongs to a Gaussian. Notice the "-" sign in the above condition, in $(1 - \epsilon_{G-U})$. Then, we expand the interval to the right with one sample. The procedure stops when $\varepsilon_G^2 \geq \varepsilon_U^2$, that is when the Gaussian approximation ceases to produce an error reduction, compared to the uniform distribution approximation.

The above procedure is applied once to each UD interval.

4. Algorithm

In this section we present the steps of the approximation algorithm with comments. Two versions of approximation are given, the second one achieving better approximations. Notice that the algorithm does not aim to determine a very good approximation, which would involve numerous functions in the G-U-MM model; in contrast, we are interested to keep the number of components of the approximation low, because one of the qualities of a good segmentation is the small number of segments. Recall that a key idea throughout this paper is to obtain a reasonable approximation that helps separate regions of the image according to their specific statistic in the hope that the probability distribution is related, in the human vision mechanism, to the segmentation. Therefore, we will allow for even poor approximations, when these keep the number of segments low and do not significantly affect the regions assigned to the segments, in the images. Some of the steps of the subsequent presentation of algorithm are illustrated in Fig. 6.

We emphasize that the algorithm presented subsequently consists only in the new section of the overall algorithm and adds to the basic section already presented in [14], [17]. The basic section of the whole algorithm determines two types of intervals, named "uniform" and "undetermined"(-type). These intervals are further processed as follows.

1. Let the interval $[x_1, x_2]$ be classified as 'undetermined-type' (Fig. 6). Determine the gray level in the center of the interval: $h(\frac{x_1+x_2}{2})$, where h is the histogram function.
   IF $h(\frac{x_1+x_2}{2}) > h(x_1)$ AND $h(\frac{x_1+x_2}{2}) > h(x_2)$ THEN go to step 2, ELSE go to step 9.

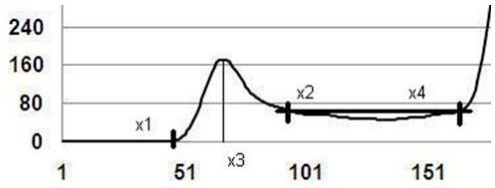

Fig. 6. Fragment of histogram.

2. Find $x_3 = argmax(h(x)), x \in [x_1, x_2]$

3. Suppose that x_3 is a Gaussian peak; then, the local approximation (denoted by h, as the histogram) $h(x) = A \cdot exp(-(x - x_3)^2/b)$. Consequently, $A = h(x_3)$.

   Comment. As suggested by Fig. 3, the suppositions made in steps 1-3 lead to a rough identification of the peak of the Gauss function, and thus, to a rough approximation. It is possible that the double condition (connected by AND) at step 1 is false, yet the interval corresponds to a Gauss peak. Step 9 is meant to correct these situations.

4. Determine b_1 optimal for the left side:
   For $b = 3$ to 7200,
   determine the error of approximation for the Gaussian distribution:
   $\varepsilon^2_{(b)} = \sum_{x_1}^{x_3}(h(x) - Ae^{(-(x-x_3)^2/b)})$.

   Find b optimal corresponding to argmin $\varepsilon^2_{(b)}$.

   Comments: the increment in the loop is 1; the dispersion needs not be an integer; the values 3 and 7200 were empirically found convenient for the images processed, but other limits may be needed for other images. Because the sum is from x_1 to x_3, the value of optimal b so determined is in fact optimized for the left side, that is, we find b_1 optimal.

5. Determine the error and b_2 optimal for the right size.

6. Determine b optimal as $b = (b_1 + b_2)/2$, and the total error $error = error_1 + error_2$, where $error_1$ and $error_2$ are those at steps 4 and 5.

   Comment. The second method for finding the value of b optimal is as follows:

   Using again $g(x) = A \cdot exp(-(x - (x_1 + x_2)/2)^2)/b$, where x_1 and x_2 are the limits of the 'undetermined-type' interval, we find for the left side of the approximating function, $g(x1) = A \cdot exp(-((x_1 - center)/2)^2)/b_1 = h[x_1]$, where '*center*' is x_3. Then,
   $-(x_1 - center)^2/b_1 = log(h[x_1]/A)$, or $b_1 = -(x_1 - center)^2/log(h[x_1]/A)$
   where b_1 is determined for $x = x_1$.

   Similarly, b_2 is determined for $x = x_2$ as
   $-(x_2 - center)^2/b = log(h[x_2]/A)$, or $b_2 = -(x_2 - center)^2/log(h[x_2]/A)$.

   Finally, consider $b = (b_1 + b_2)/2$. (End of the variant method and of the comment.)

7. Compute the error $\varepsilon^2_{(b)} = \sum_{x_1}^{x_3}(h(x) - A \cdot e^{-(x_i - center)^2/b})$, as for step 6.

8. Compare b optimal determined at step 6 with the first method with that determined by the second method, based on the corresponding errors computed at step 7. Choose b that corresponds to the smaller error (for each b optimal we compute the errors at steps 6 and 7).

   Comment. The above steps determine and approximate only the "top" of the Gaussians, that is the portions of the Gaussians that are erroneously detected as "uniform" intervals. For the ascending and respectively descending segments of Gaussians that are left as "undecided" at the detection of the UD intervals, the subsequent steps are used.

9. For intervals declared as uniform in the first stage of the algorithm, when they do not satisfy the condition at step 2, proceed as follows. Using an overlapping

window of 24 gray levels on the histogram, IF the average of 6 gray levels from the center is larger than the average of 6 gray levels from the left AND average of 6 gray levels from the center is larger than the average of 6 gray levels from the right, then the interval is a Gaussian one, ELSE, the interval is considered constant (UD). For new Gaussian intervals, go to step 4 and determine the optimal b and compute the error according to steps 4-6.

Comment. The next step in the algorithm decides if pixels at the boundaries of the Gauss intervals, belonging to UD intervals, should or should not be merged to the G intervals. The decision is made based on the minimal approximation error.

10. Increment with 1 the interval of the Gaussian at the left side; compute the error for Gaussian and uniform distribution. If the error for the Gaussian is smaller, then we attach that gray level value to the Gaussian interval; if not, it remains in the UD interval and no more interval enlargements are tried at left. Then, check in the same way to the right side. If the unit enlargement of the interval was accepted at left or right, then, we obtain and keep the new G and UD intervals, that is, the new segmentation thresholds.

Hybrid mixtures may be expressed as mixtures of distributions on disjoint intervals that are forming a partition of the [0,255] gray level interval. Alternatively, they can be additive mixtures, with distributions superposing on some intervals. The Gaussian mixture models assume additive mixtures with distributions superposed on the whole [0, 255] interval. Obviously, assuming total superposition simplifies the mathematical approach in the approximation, but produces the convolution of the probability distribution functions. We are not aware of any paper questioning the suitability of such an approach from the point of view of the human observer. Moreover, we draw the attention on the lack of evidence for supporting the suitability of GMM (Gauss superposition model) for images, beyond pure technical convenience. Consider for example a single object with uniform gray level in a small interval of values, over a uniformly distributed background. The two parts of the image, object and background, are in no way correlated, moreover no gray level value of one image is present in the other object; in this case, no superposition occurs. Another example of image where the composing distributions may be considered non-superposing, truncated Gaussians and zero-levels on the histogram on extended intervals is the *rabbit toy* in Fig. 7.

Fig. 7. Original image *rabbit* [22] 170×170 pixels.

5. Results

The previous sections presented the method and the algorithm for histogram representation as a piecewise function. The key issue was the determination of the G and UD intervals for the piecewise representation. In turns, these intervals are assumed to define the gray level segments in the image, which is the basic idea of the algorithm. Partial and preliminary results presented here were recently presented in [34].

Table 1 summarizes a set of results, including the filtered histograms, the corresponding images, the histogram approximants, and the corresponding segmented images. It is striking to note that *Lena* image seems to be the worst approximated, because of its intricacies, yet the segmentation obtained is one of the best, compared to the segmentation by Otsu's method. Also notice on *Lena* picture that part of the mixture of Gaussians is approximated with a staircase function. The same happens for other histograms, especially when two Gauss functions overlap heavily.

Table 1a. Segmented images with both methods [*Lena*]

Original filtered histogram with thresholds set for the first method (3 segments)	Segmented image with the first method
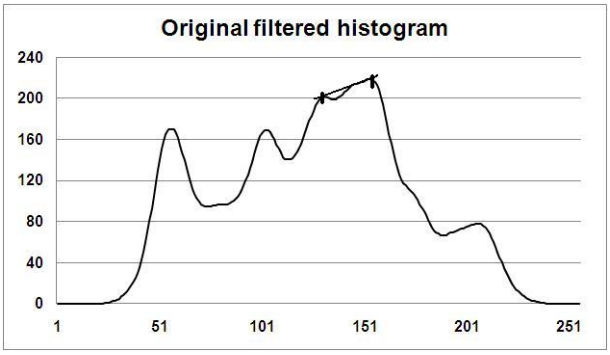	
Original and new obtained histogram (6-8 segments)	Segmented image with the new method
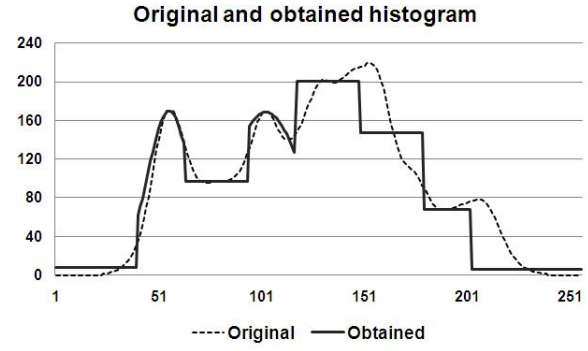	

Table 1b. Segmented images with both methods [*Peppers, Rabbit*]

Original filtered histogram with thresholds set for the first method (3 segments)	Segmented image with the first method
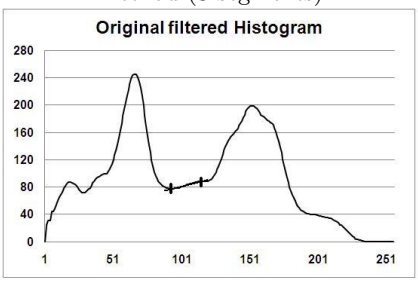	
Original and new obtained histogram (6-8 segments)	Segmented image with the new method
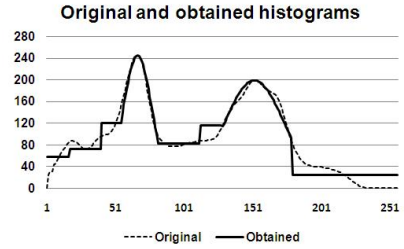	
Original filtered histogram with thresholds set for the first method (3 segments)	Segmented image with the first method
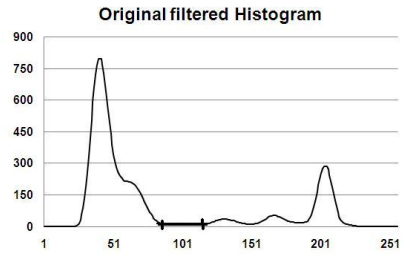	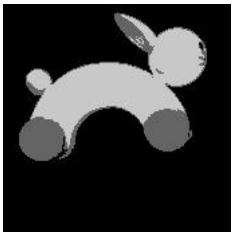
Original and new obtained histogram (6-8 segments)	Segmented image with the new method
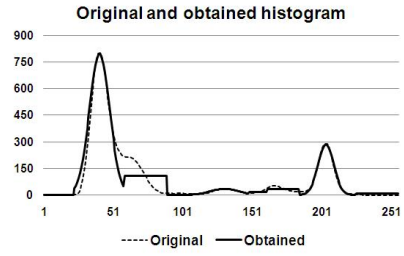	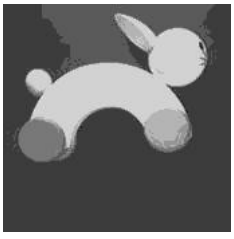

Table 1c. Segmented images with both methods [*Blood Cells*]

Original filtered histogram with thresholds set for the first method (3 segments)	Segmented image with the first method
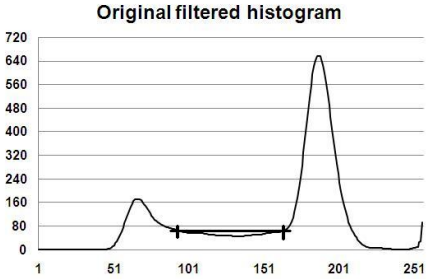	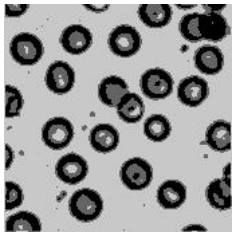
Original and new obtained histogram (6-8 segments)	Segmented image with the new method
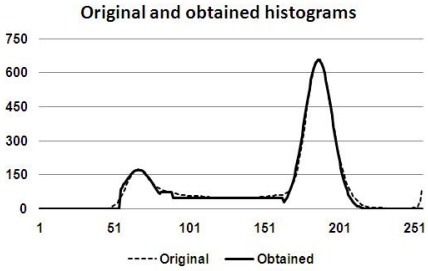	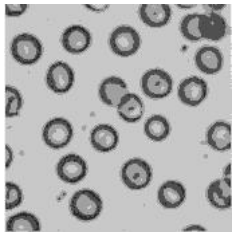

The segmentation results obtained with the improved GUMM algorithm presented in this paper are visibly better than the ones obtained with the previous version we reported. However, we compromised between the complexity of the model, which is represented by the number of Gaussian and uniform distributions in the mixture, and the computational load. Therefore, as the approximated histograms show, the approximation is imperfect, especially in some intervals of the gray levels. For example, for the images 'Lena', 'peppers', and 'rabbit', sub-intervals that belong to regions of Gaussian distributions are approximated with uniform distributions.

6. Objective assessment of the segmentation quality

The comparison of the results obtained with the proposed segmentation method with the results obtained with other methods is performed by means of several objective segmentation quality indexes, following the literature [27], [28], [29], [30], [31]. The indexes we use are briefly presented below, paraphrasing the literature [27]-[31]. Notice that the smaller is the index, the better the segmentation is considered; large numbers of segments are penalized by all indices; the criteria F_1 and Q below also penalize too large segments.

1. Liu and Yang's evaluation index is:

$$F = \sqrt{N} \sum_{j=1}^{N} e_j^2 / \sqrt{S_j}, \tag{8}$$

where N is the number of obtained regions after segmentation, S_j is the area of region j, and e_j^2 is the squared color error (or the gray level). The error is computed as:

$e_j^2 = \sum_{k \in S_j} (x_k - \overline{x})^2$,

where x_k is the gray level of the pixel, and the $\overline{x}$ is the average gray level of the region.

2. Borsotti, Campadelli and Schettini's in function F_1 improves Liu and Yang's method:

$$F_1 = 1/(1000 \cdot S_I) \cdot \sqrt{\sum_{a=1}^{MaxArea} [N(a)]^{1+1/a}} \sum_{j=1}^{N} \varepsilon_j^2 / \sqrt{S_j}, \tag{9}$$

where S_I is the image surface, $N(a)$ denotes the number of regions in the segmented image having an area exactly a, and $MaxArea$ is the area of the largest region in the segmented image.

3. Borsotti's criterion is based on the value of the parameter Q,

$$Q = (1/(10000) \cdot S_I) \cdot \sqrt{N} \sum_{j=1}^{N} (\varepsilon_j^2 / (1 + \log S_j) + N(S_j)/S_j)^2), \tag{10}$$

where $N(S_j)$ denotes the number of regions in the segmented image having an area exactly S_j.

4. The intra-region uniformity criterion of Levine and Nazif [31] is:

$$Lev = \sum_j \sum_{x \in R_j} (f(x) - 1/S_j \sum_{x \in R_j} f(x))^2 = \sum_j \sigma_j^2 / C. \tag{11}$$

Above, $f(x)$ is the intensity of the pixel x, and C is a normalization coefficient, equal to the maximum possible variance:

$C = (f_{max} - f_{min})^2/2$.

5. Entropy-based evaluation method [30]. It is well-known that the entropy is a measure of the disorder; in this case, it applies to the disorder within a region of the image. As such, it may be used as a feature of the segments and therefore can be used in the segmentation quality assessment. The entropy for the region j is defined as:

$$H_v(R_j) = -\frac{L_j(m)}{S_j} \cdot \log\left(L_j(m)/S_j\right), \tag{12}$$

where $L_j(m)/S_j$ represents the probability that a pixel in region R_j has a luminance value of m. The notation $H_v(R_j)$ was simplified to $H(R_j)$ with the default feature v being luminance. H. Zhang et al. define the expected region entropy of image I:

$$H_r(I) = \sum_{j=1}^{N} (S_j/S_I) H(R_j), \tag{13}$$

and the layout entropy:

$$H_l(I) = -\sum_{j=1}^{N} (S_j/S_I) \log(S_j/S_I), \tag{14}$$

These authors propose in [30] to combine both the layout entropy and the expected entropy in measuring the effectiveness of a segmentation method:

$$E = H_l(I) + H_r(I). \tag{15}$$

Table 2. Evaluation of the segmented images

	Lena	*Peppers*	*Rabbit*	*Blood cells*
Initial proposed method	$F \simeq 215677$	$F \simeq 216562$	$F \simeq 89900$	$F \simeq 107778$
Improved method	$F \simeq 73157$	$F \simeq 109499$	$F \simeq 52371$	$F \simeq 132450$

Table 3a. Evaluation and comparison of segmented images [*Lena*, *Peppers*, *Rabbit*, *Blood cells*]

	Lena	*Peppers*	*Rabbit*	*Blood cells*
Improved proposed method	F= 73157 F1=0.0025 Q=0.0036 Lev=0.68 E=6.90	F=109499 F1= 0.0038 Q=0.0053 Lev=0.91 E=6.85	F = 52371 F1= 0.0018 Q=0.0036 Lev=0.62 E=6.27	F=132450 F1= 0.0046 Q=0.0074 Lev=0.62 E=7.22
Otsu's method	F=86556 F1=0.0030 Q=0.0043 Lev=0.69 E=6.99	F=79540 F1=0.0028 Q=0.0035 Lev=0.84 E=6.65	F=45386 F1=0.0016 Q=0.0020 Lev=0.68 E=6.25	F=79618 F1=0.0028 Q=0.0058 Lev=0.55 E=7.48

Table 3b. Evaluation and comparison of segmented images [*Giraffe1* [32], *Girafe2*, *Skier* [33]]

	Giraffe1 [32]	*Girafe2*	*Skier* [33]
Improved proposed method	F=176239 F1= 0.0115 Q=0.0163 Lev=0.13 E=8.02	F=95351 F1=0.0033 Q=0.0056 Lev=0.77 E=6.93	F =188243 F1=0.0075 Q=0.0104 Lev=0.74 E=7.42
Otsu's method	F=167272 F1=0.0109 Q=0.0145 Lev=0.13 E=7.97	F=68262 F1=0.0024 Q=0.0034 Lev=0.74 E=6.99	F=167367 F1=0.0066 Q=0.0083 Lev=0.75 E=7.30

The results of the segmentation of several images with the presented method and the results of the segmentation with Otsu's method were assessed according to the indexes presented above. The results of the evaluation are listed in the Tables 2 and 3. Table 2 compares the preliminary version of the segmentation algorithm [34] and the current one. The assessment was performed using a single criterion.

7. Conclusions

We suggested that using mixtures of two elementary distributions for modeling the distribution of the gray levels or colors in an image, a simpler way of approximation of the histogram is obtained that, moreover, allows obtaining better segmentation results. In addition, segmentation results sometimes are closer to the semantic content in the image. The specific mixed distribution proposed in the context of image segmentation is the G-U-MM one. Its choice was based on empirical analysis of a set of image histograms.

We presented detailed explanation for the rationale of the G-U-MM models proposed as a foundation of the segmentation process. The proposed segmentation procedure is directly based on the G-U-MM class of models. A piecewise approximation was used for the histogram; the piecewise representation directly connects to the segmentation.

The algorithms given are computationally efficient. The basic algorithm is semi-heuristic because while it has its roots in function approximation, at a certain level of the refining of the approximation it uses heuristics to reduce the computational load. Compared to the method proposed in our previous papers on the subject, we shown the correctness of the procedure and we improved it to remove the confusion between top of Gaussians with large spreading and a uniform distribution. The algorithm will be deposited with CERFS (web page) and is available for research purposes.

The analysis of the segmentation results was performed by computing objective quality metrics. The comparison of the values of these indices as obtained with the proposed method and as obtained with Otsu's segmentation shows that the segmentation is improved by the use of G-U-MM method for some typical images, but not for

all. This is natural, as the GUMM model covers in an efficient manner (*i.e.*, with few Gaussians and few uniform distributions) only a subclass of images. Choosing a suitable model (approximation) of the image statistics between different possible models, for example between GMMs and GUMMs, must guide what images are suitable for segmentation with the GUMM method.

Acknowledgment. This research was not asked for or supported by any institution; most of the conceptual work was benevolently performed by HNT. The experiments were made during MR's PhD research internship at the Technical University "Gh.Asachi" of Iasi; the scholarship was offered by the Romanian Governement and was managed by the Francophone University Agency (AUF). MR thanks AUF for this support.

The work relates to the research project *Cognitive Systems* developed in the frame of the Romanian Academy. The authors vividly thank colleagues Adrian Ciobanu and Silviu Bejinariu and Prof. H. Costin for very careful corrections of preliminary versions of the paper.

Authors' contributions. H.-N. Teodorescu has written the paper, except Sections 5–6, and proposed the research topic, the approach, the models, the method of solving the segmentation, the algorithms; he interpreted most of the results and derived conclusions. M. Rusu wrote the code, for which she alone assumes responsibility, performed simulations and experiments, contributed to the interpretation of the results, wrote the sections 6 on objective assessment of the segmentation quality, and alone produced the largest part of processed images. Both authors discussed the paper and agreed with its final form.

References

[1] Kanga C. C., Wang W. J., Kang C. H., *Image segmentation with complicated background by using seeded region growing*, Int. J. Electronics and Communications, Vol. **66**, No. 9, 2012, pp. 767–771.

[2] Jellema A. *et al.*, *Landscape character assessment using region growing techniques in geographical information systems*, J. Environmental Management, Vol. **90**, No. 2, 2009, pp. 161–174.

[3] Liu L., Sclaroff S., *Deformable model-guided region split and merge of image regions*, Image and Vision Computing, Vol. **22**, No. 4, 2004, pp. 343–354.

[4] Cai W., Chen S., Zhang D., *Fast and robust fuzzy c-means clustering algorithms incorporating local information for image segmentation*, Pattern Recognition, Vol. **40**, No. 3, 2007, pp. 825–838.

[5] Chen Y. B., *A robust fully automatic scheme for general image segmentation*, Digital Signal Processing, Vol. **21**, No. 1, 2011, pp. 87–99.

[6] Tobias O. J., Seara R., *Image segmentation by histogram thresholding using fuzzy sets*, IEEE Trans. Image Processing, Vol. **11**, No. 12, 2002, pp. 1457–1465.

[7] Hammouche K., Diaf M., Siarry P., *A multilevel automatic thresholding method based on a genetic algorithm for a fast image segmentation*, Computer Vision and Image Understanding, Vol. **109**, No. 2, 2008, pp. 163–175.

[8] Felzenszwalb P. F., Huttenlocher D. P., *Efficient graph-based image segmentation*, Int. J. Computer Vision, Vol. **59**, No. 2, 2004, pp. 167–181.

[9] Costin H., *A fuzzy rules-based segmentation method for medical images analysis*, Int. J. Comput. Commun., Vol. **8**, No. 2, pp. 196–205, April 2013.

[10] Povey D., Burget L. *et al.*, *Subspace Gaussian mixture models for speech recognition*, Proc. ICASSP, 2010, pp. 4330–4333.

[11] Kumar G. S. *et al.*, *Speaker recognition using GMM*, Int. J. Engineering Science and Technology Vol. **2**(6), 2010, pp. 2428–2436.

[12] Vondra M., Vich R., *Evaluation of speech emotion classification based on GMM and data fusion, Cross-Modal Analysis of Speech, Gestures, Gaze and Facial Expressions*, Springer Berlin Heidelberg, 2009, pp. 98–105.

[13] Liu J., Zhang H., *Image segmentation using a local GMM in a variational framework*, J. Mathematical Imaging and Vision, Vol. **132**, No. 46, 2012, pp. 1992–2013.

[14] Teodorescu H.-N., Rusu M., *Image segmentation based on G-UN-MMs and heuristics - Theoretical background and results*, Proc. Romanian Academy Series A, Vol. 14, No. 1, 2013, pp. 78–85.

[15] Rasmussen C. E., Williams C. K. I., *Gaussian processes for machine learning*, the MIT Press, 2006, Massachusetts Institute of Technology, Chapter 3, `http://www.gaussianprocess.org/gpml/chapters/RW3.pdf`

[16] Blanchard G., Kawanabe M. *et al.*, *In Search of non-Gaussian components of a high-dimensional distribution*, J. Machine Learning Research, Vol. **7**, 2006, pp. 247–282.

[17] Teodorescu H.-N., Rusu M., *Yet another method for image segmentation based on histograms and heuristics*, Computer Science J. of Moldova, Vol. **20**, No. 2(59), 2012, `http://www.math.md/publications/csjm/issues/v20-n2/11087/`

[18] Verikas A., Malmqvist K., Bergman L., *Colour image segmentation by modular neural network*, Pattern Recognition Letters, Vol. **18**, No. 2, 1997, pp. 173–185.

[19] Image *blood cells*. Available at: `http://www.pudn.com/downloads58/sourcecode/math/detail206012.html` (Last time accessed 10 March 2013)

[20] Image *Lena*. Available at: `http://www.ece.rice.edu/ wakin/images/lena512.bmp`

[21] Image *peppers*. Available at: `http://introcs.cs.princeton.edu/java/31datatype/peppers.jpg`

[22] Image *rabbit*. Available at: `http://www.engineering.uiowa.edu/ dip/examples/images/rabbit.jpg`

[23] Duvenaud D., Nickisch H., Rasmussen C. E., *Additive Gaussian processes*, 2011, Available: COPE: `http://arxiv.org/pdf/1112.4394v1.pdf`

[24] Liu J., Yang Y.-H., *Multi-resolution color image segmentation*, IEEE Trans. Pattern Analysis and Machine Intelligence, Vol. **16**, No. 7, 1994, pp. 689–700.

[25] Bejinariu S.I., Rotaru F., Nita C.D., *Information fusion techniques for segmentation of multispectral images*, Memoirs of the Scientific Sections of the Romanian Academy, Tome **XXXV**, 2012, pp. 125–143.

[26] Garcia D., *Otsu's method*. Available at: `http://www.mathworks.com/matlabcentral/fileexchange/26532-image-segmentation-using-otsu-thresholding/content/otsu.m`

[27] Zhang H. *et al.*, *Image segmentation evaluation: A survey of unsupervised methods*, Computer Vision and Image Understanding, Vol. **110**, No.2, 2008, pp. 260–280.

[28] Udupa K. *et al.*, *A framework for evaluating image segmentation algorithms*, Computerized Medical Imaging and Graphics, Vol. **30**, 2006, pp. 75–87.

[29] Chabrier S., Emile B., Rosenberger C., Laurent H., *Unsupervised performance evaluation of image segmentation*, EURASIP J. Applied Signal Processing, Vol. **2006**, 2006, pp. 1–12.

[30] Zhang H., Fritts J. E., Goldman S. A., *An entropy-based objective evaluation method for image segmentation*, Proc. IST-SPIE Storage and Retrieval Methods and Applications for Multimedia, 2004, Vol. **5307**, pp. 38–49.

[31] Philipp-Foliguet S., Guigues L., *Multi-scale criteria for the evaluation of image segmentation algorithms*, J. Multimedia, Vol. **3**, No. 5, 2008, pp. 42–56.

[32] Berry P. S. M., Bercovitch F. B., *Darkening coat colour reveals life history and life expectancy of male thornicrofts giraffes*, J. Zoology, Vol. **257**, 2012, pp. 157–160.

[33] Berkeley segmentation dataset. Available at: `http://www.eecs.berkeley.edu/Research/Projects/CS/vision/bsds/BSDS300/html/dataset/images/gray/61086.html`

[34] Rusu M., Teodorescu H.-N., *Quality Analysis of Image Segmentation based on G-UN-MMS*, Proc. 2nd Int. Conf. Nanotechnologies and Biomedical Engineering, Chişinău, Republic of Moldova, April 18-20, 2013, pp. 620–624.